clean with nonuniform burning, with some pronounced dips and rises.

Overall, there is a good qualitative correlation between the predicted augmented pressure curve and the static firing data of Ref. 4. Because of nozzle throat erosion later in the experimental firing, the predicted peak pressure is somewhat higher than expected (no throat erosion modeled). Similarly, for the flight case with increasing forward acceleration and spin as the firing proceeds, the predicted pressure peaks somewhat higher than expected relative to the reported data of Ref. 4. Only later into the flight does the normal acceleration of the motor rotation begin to dominate the lateral and longitudinal acceleration components in affecting the combustion process.

References

[1]Greatrix, D. R., "Parametric Analysis of Combined Acceleration Effects on Solid-Propellant Combustion," *Canadian Aeronautics and Space Journal*, Vol. 40, No. 2, 1994, pp. 68–73.

[2]Hejl, R. J., and Heister, S. D., "Solid Rocket Motor Grain Burnback Analysis Using Adaptive Grids," *Journal of Propulsion and Power*, Vol. 11, No. 5, 1995, pp. 1006–1011.

[3]Greatrix, D. R., Gottlieb, J. J., and Constantinou, T., "Quasi-Steady Analysis of the Internal Ballistics of Solid-Propellant Rocket Motors," *Canadian Aeronautics and Space Journal*, Vol. 33, No. 2, 1987, pp. 61–70.

[4]Lucy, M. H., "Spin Acceleration Effects on Some Full-Scale Rocket Motors," *Journal of Spacecraft and Rockets*, Vol. 5, No. 2, 1968, pp. 179–183.

Propellant Design Relationships for Throttled Gas Generators

R. A. Frederick Jr.*
University of Alabama in Huntsville, Huntsville, Alabama 35899
and
Iwao Komai†
NOF Corporation, Taketoyo, Achii 470-23, Japan

Nomenclature

A_b = propellant burn surface area
a = burning rate coefficient
a' = burning rate coefficient at reference pressure and temperature
c^* = propellant characteristic exhaust velocity
K = burn area over throat area
$\dot{m}_f$ = mass flow rate of fuel
N_{MAX} = maximum allowable pressure sensitivity
n = pressure exponent
P = chamber pressure
P' = chamber pressure over reference pressure
r = propellant burn rate
T_i = initial propellant temperature
α = temperature sensitivity coefficient
α' = temperature sensitivity coefficient at reference pressure
ρ_p = propellant density

Subscripts
r = reference conditions
s = standard conditions
1 = maximum limit
2 = minimum limit

Received Aug. 25, 1994; revision received Nov. 2, 1995; accepted for publication Nov. 28, 1995.

*Assistant Professor, Department of Mechanical and Aerospace Engineering, Propulsion Research Center. Senior Member AIAA.

†Senior Research Engineer. Member AIAA.

Introduction

WHEN formulating gas generator propellants, the designer must achieve a specified mass flow schedule. One approach is to use propellants with large pressure sensitivity and a variable-area nozzle. This promotes substantial variations in mass flow while maintaining a reasonable pressure range. The propellant temperature sensitivity and combustion efficiency are additional factors that influence the design. The objective of this work is to calculate a propellant solution space that fulfills the design requirements for a variable-flow gas generator. The scope includes 1) developing a design methodology that incorporates mass flow rate, pressure, and temperature requirements; 2) deriving design equations for propellants with temperature-dependent pressure exponents; and 3) calculating regions of compliant propellant ballistics for an example ducted rocket application.

Approach

Gas Generator Constraints

The gas generator design is assumed to be bounded by mass flow rate, propellant temperature, and chamber pressure requirements. The mass flow rate range of a ducted rocket motor can be determined from anticipated altitude, flight Mach number, and operational oxidizer-to-fuel ratio considerations: $\dot{m}_{f1} \leq \dot{m}_f \leq \dot{m}_{f2}$. The gas generator must deliver this entire range. The operating environment dictates a range of initial propellant temperatures: $T_{i,1} \leq T \leq T_{i,2}$. The maximum chamber pressure is defined by structural/weight considerations of the missile. The minimum pressure could be guided by either the choked-flow or propellant extinguishment: $P_1 \leq P \leq P_2$. It is not required that this pressure range be spanned, but the pressure limits must not be violated.

For steady-state operation, the propellant burning rate range is derived from extreme values of the required mass flow rate and the propellant burn surface area by

$$r_2 = \dot{m}_{f\,\max}/\rho_p A_{b\,\min} \tag{1}$$

$$r_1 = \dot{m}_{f\,\min}/\rho_p A_{b\,\max} \tag{2}$$

A stable equilibrium chamber pressure also requires the pressure exponent must be less than one.

Figure 1 shows how these burn rate, pressure, and pressure-exponent limits form a parallelogram-shaped region (A–B–C–D) of compliant burn rate/pressure combinations. Initial temperature effects are illustrated by two propellant burn rate curves. The maximum temperature curve intersects point A, while the minimum temperature curve intersects point C. Expressing these design criteria mathematically, we have

$$r(P_1, T_2) \leq r_1 \quad \text{and} \quad r(P_2, T_1) \geq r_2 \tag{3}$$

and $n < 1$.

Mathematical Derivations

Propellant burning rate is assumed as a function of pressure and temperature with

$$r = a_s \exp[\alpha(T_i - T_{i,s})]P^{[n_s+\beta(T_i-T_{i,s})]} \tag{4}$$

Small variations in β will result in large changes in burning rate at operational pressures. Normalizing with a reference pressure P_r, at which the contribution of the β term is zero, yields,

$$r = a_s' \exp[\alpha'(T_i - T_{i,s})]P'^{[n_s+\beta(T_i-T_{i,s})]} \tag{5}$$

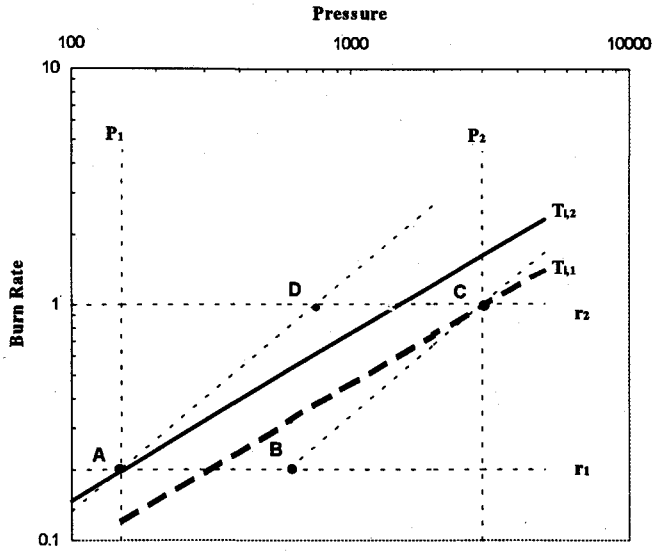

Fig. 1 Ballistics limitations diagram.

where $a_s' = r(P_r, T_{i,s})$ and $P' = P/P_r$, making $\alpha' = \alpha + \beta \ln P_r$. Normalizing makes α' the temperature sensitivity at the reference pressure. Changes in β then rotate each constant-temperature burn rate line about the point that it intersects the reference pressure.

Propellant Design Relationships

Equations to define a burning-rate, pressure-exponent solution space are now developed that satisfy the design constraints. Three limiting conditions are examined: condition I, the minimum exponent propellant sketched in Fig. 1; condition II, the maximum exponent propellant that overlays line A–D in Fig. 1; and condition III, the maximum exponent propellant that overlays line B–C in Fig. 1.

The range of acceptable pressure exponents for condition I is found by substituting Eq. (5) into Eqs. (3), yielding,

$$n_s \leq \frac{\ln r_1 - \ln a_s'}{\ln P_1'} - \frac{T_{i,2} - T_{i,s}}{\ln P_1'}\alpha' - (T_{i,2} - T_{i,s})\beta \quad (6)$$

$$n_s \geq \frac{\ln r_2 - \ln a_s'}{\ln P_2'} - \frac{T_{i,1} - T_{i,s}}{\ln P_2'}\alpha' - (T_{i,1} - T_{i,s})\beta \quad (7)$$

The reference burning rate for condition I is found by equating Eqs. (6) and (7) and solving

$$\ln a_s'|_{\mathrm{I}} = A_a^{\mathrm{I}} - B_a^{\mathrm{I}}\alpha' - C_a^{\mathrm{I}}\beta \quad (8)$$

where

$$A_a^{\mathrm{I}} = \frac{\ln P_2' \ln r_1 - \ln P_1' \ln r_2}{\ln P_2' - \ln P_1'} \quad (8a)$$

$$B_a^{\mathrm{I}} = \frac{\ln P_2'(T_{i,2} - T_{i,s}) - \ln P_1'(T_{i,1} - T_{i,s})}{\ln P_2' - \ln P_1'} \quad (8b)$$

$$C_a^{\mathrm{I}} = \frac{\ln P_1' \ln P_2'(T_{i,2} - T_{i,1})}{\ln P_2' - \ln P_1'} \quad (8c)$$

Substituting Eqs. (8) into either Eq. (6) or (7) yields the minimum exponent as a function of α and β:

$$n_s|_{\mathrm{I}} = A_n^{\mathrm{I}} + B_n^{\mathrm{I}}\alpha' + C_n^{\mathrm{I}}\beta \quad (9)$$

where

$$A_n^{\mathrm{I}} = \frac{\ln r_2 - \ln r_1}{\ln P_2' - \ln P_1'} \quad (9a)$$

$$B_n^{\mathrm{I}} = \frac{T_{i,2} - T_{i,1}}{\ln P_2' - \ln P_1'} \quad (9b)$$

$$C_n^{\mathrm{II}} = \frac{\ln P_1'(T_{i,2} - T_{i,s}) - \ln P_2'(T_{i,1} - T_{i,s})}{\ln P_2' - \ln P_1'} \quad (9c)$$

Now, substituting $n_{s\max}$ into Eqs. (6) and (7) gives equations for the reference burning rate at conditions II and III.

$$\ln a_s'|_{\mathrm{II}} = \ln r_2 - n_{s\max} \ln P_2' - (T_{i,1} - T_{i,s})(\alpha' + \beta \ln P_2') \quad (10)$$

$$\ln a_s'|_{\mathrm{III}} = \ln r_1 - n_{s\max} \ln P_1' - (T_{i,2} - T_{i,s})(\alpha' + \beta \ln P_1') \quad (11)$$

where $n_{s\max}$, the maximum allowable standard exponent, and N_{MAX}, the overall maximum exponent that the designer allows, are related by

$$n_{s\max} = N_{\mathrm{MAX}} \leq 1.0, \quad \text{if} \quad \beta = 0 \quad (12a)$$

$$n_{s\max} = N_{\mathrm{MAX}} - \beta(T_{i,2} - T_{i,s}), \quad \text{if} \quad \beta > 0 \quad (12b)$$

$$n_{s\max} = N_{\mathrm{MAX}} - \beta(T_{i,1} - T_{i,s}), \quad \text{if} \quad \beta < 0 \quad (12c)$$

Equations (8–12) now define the reference propellant burning rate a_s' and its corresponding reference exponent n_s as functions of α' and β.

Results for an Example Application

An example application is now shown for a ducted rocket gas generator. Table 1 lists the selected and derived parameters for the application. An 8.0-in.-diam, end-burning gas generator was assumed to operate over a Mach number range of 2.5–3.5, at altitudes from 6500 to 65,000 ft. Other assumptions include 1) the reference pressure is 1000 psia, 2) the reference temperature is 65°F, and 3) $N_{\mathrm{MAX}} = 1.0$. The effect of temperature sensitivity parameters α' and β on the resulting a_s' vs n_s solution space will now be presented and discussed for this application.

Conventional Propellants: Effect of α when $\beta = 0$

The design relationships are first applied to conventional propellants that have no pressure exponent sensitivity ($\beta = 0$). Figure 2a is a propellant diagram that describes the region of acceptable burn rate properties as a function of increasing α' (equivalent to conventional propellant temperature sensitivity for this case). The x axis represents the propellant burning rate at the reference pressure ($P_r = 1000$ psia) and reference temperature ($T_{i,s} = 65$°F). The y axis represents the corresponding burn rate exponent at the reference temperature n_s.

The $\alpha = 0$ case shows the largest area of ballistic properties that will satisfy the gas generator constraints. The solution space is a triangular region with vertices at condition I [defined by Eqs. (8) and (9)], condition II [defined by Eqs. (10) and (12a)], and condition III [defined by Eqs. (11) and (12a)]. Condition I represents the reference burning rate for the minimum

Table 1 Baseline ducted rocket gas generator

Selected	Derived
$\dot{m}_{\min} = 0.48$ lbm/s	$r_1 = 0.20$ in./s
$\dot{m}_{\max} = 3.26$ lbm/s	$r_2 = 1.00$ in./s
$T_1 = -15$°F	$A_a^{\mathrm{I}} = -0.5902$
$T_2 = 145$°F	$B_a^{\mathrm{I}} = -21.32$
$P_1 = 150$ psia	$C_a^{\mathrm{I}} = -111.31$
$P_2 = 3000$ psia	$A_n^{\mathrm{I}} = 0.5372$
$A_b = 50.27$ in.^{2}	$B_n^{\mathrm{I}} = 53.4$
$N_{\mathrm{MAX}} = 1.0$	$C_n^{\mathrm{I}} = -21.4$
$\rho_p = 0.047$ lb/in.^{3}	——

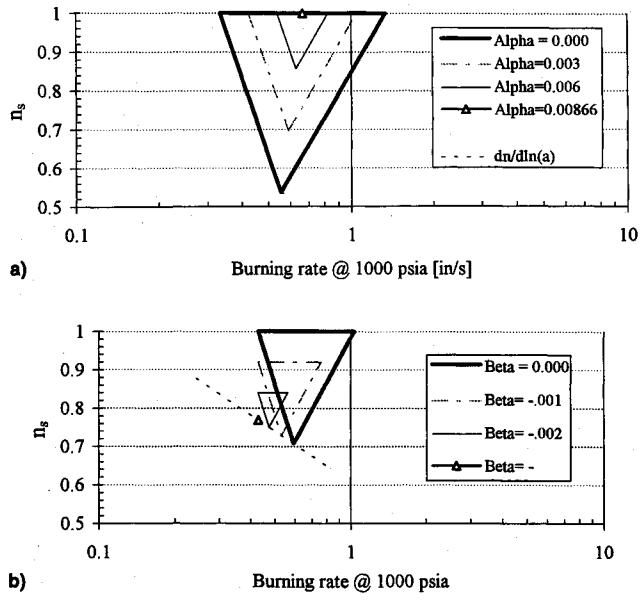

Fig. 2 Propellant ballistics diagram: a) $\alpha = 0.6-0.00866$, $\beta = 0.000$ and b) $\alpha = 0.00318$, $\beta = 0$ to -0.00289.

exponent propellant that satisfies the constraints. The maximum exponent N_{MAX} and standard exponent n_s are identical in this case.

As α' is increased, the triangular region becomes smaller. The minimum exponent increases until the burn rate curves span from line A–C to line B–D in Fig. 1, in which case

$$\alpha'_{MAX} = (N_{MAX} - A^I_n)/B^I_n, \qquad @(\beta = 0) \qquad (13)$$

giving the value of 0.00866 1/°F, which is plotted as the center point of Fig. 2a.

Effect of β at Constant α'

Figure 2b illustrates the effects of variations in the pressure exponent sensitivity for a fixed value of α'. In this case, α' is assumed constant at 0.00318 1/°F, while the exponent sensitivity ranges from 0 to −0.00289 1/°F. The variation in exponent sensitivity causes a reduction of the triangular solution space until it becomes a point at the maximum allowable value. The minimum exponent increases while its corresponding reference burning rate decreases.

Increasing the pressure exponent sensitivity then reduces and translates the propellant solution space to narrower exponent ranges and lower reference burning rates. The maximum value of pressure exponents also decreases as β increases [Eq. (12b)].

Conclusions

Propellant design relationships for variable exponent propellants have been developed and applied to a gas generator design problem. The method defines a region of acceptable propellant ballistic properties as a function of two propellant temperature sensitivity parameters. The design achieves mass flow rate, pressure, pressure exponent, and temperature range constraints. The propellant diagram approach gives the designer or propellant formulator a region of compliant ballistic properties for a given application instead of a single design point.

Acknowledgment

This work was sponsored by the Propulsion Research Center at the University of Alabama in Huntsville.

Effects of Kevlar® Fibers on Ammonium Perchlorate Propellant Combustion

M. H. Hites*
Illinois Institute of Technology, Chicago, Illinois 60616
and
M. Q. Brewster†
University of Illinois at Urbana–Champaign, Urbana, Illinois 61801

Introduction

MICROSCOPIC chopped Kevlar fibers were added to ammonium perchlorate (AP) composite propellants to investigate their burn rate enhancing features. Kevlar fibers have been used in the past[1] to increase the strength of AP composite propellants, but as a side effect it was observed that the fibers increased the burning rate of an AP/Al composite as much as 27% at 3.5 MPa. In the present work, steady burning rate measurements and combustion photography were used to quantify the burning rate enhancement and suggest a possible explanation for the observed increases.

Experimental

The steady burning rate was measured for the series of AP composite propellants shown in Table 1. The burning rate of each propellant was measured using the fuse wire technique in a nitrogen-purged combustion bomb. Strands of 7 × 7 mm cross section and 30–60 mm length were coated lightly with vacuum grease as an inhibitor and were ignited by nichrome wire. The initial temperature of strands was ambient room temperature (20–25°C).

High-speed and microscope photography were used to investigate the qualitative differences between the gas phase combustion and surface condition of the various propellants. Conventional VHS camcorder movies and 35-mm SLR macrolens photography were also used to reveal macroscopic differences between the propellants. Although only photographs from the 35-mm photography are presented here, some observations based on the other photographic techniques are discussed when applicable.

Results

Burning rate measurements of the nonmetallized propellants are shown in Fig. 1 along with the corresponding burning rate equation:

$$r = aP^n$$

where burning rate r is in mm/s and pressure P is in MPa. The coefficient a and exponent n were determined by a least-squares fit, and a linear correlation coefficient of 0.98 or better was calculated for each of the curve fits. Figure 1a shows that the addition of small amounts of Kevlar increased the burning rate and lowered the burning rate exponent slightly in nonmetallized AP systems. Figure 1b compares propellants with fiber lengths of 2 and 5 mm to a fiberless AP composite propellant and demonstrates increased burning rate with increased

Received Sept. 28, 1994; revision received April 26, 1995; accepted for publication Sept. 11, 1995.

*Research Assistant, Department of Mechanical and Aerospace Engineering, 10 West 32nd Street. Student Member AIAA.

†Professor, Department of Mechanical and Industrial Engineering, 1206 West Green Street. Associate Fellow AIAA.